Electronic supplementary information

Photoreductive Electron Transfers in Nanoarchitectonics Organization between a Diketopyrrolopyroleplatinum(II)-Containing Organometallic Polymer and Various Electron Acceptors

Gabriel Marineau-Plante,[a] Malak Qassab,[b] Adrien Schlachter,[a] Mélodie Nos,[b] Muriel Durandetti,[c] Julie Hardouin,[d,e] Cyprien Lemouchi,*[b] Loïc Le Pluart,*[b] Pierre D. Harvey,*[a]

[a]*Département de chimie, Université de Sherbrooke, Sherbrooke, PQ, Canada J1K 2R1. E-mail: Pierre.Harvey@USherbrooke.ca*

[b] *Normandie Univ, LCMT UMR 6507, ENSICAEN, UNICAEN, CNRS, 6 Bd. du Maréchal Juin, 14050 Caen, France. E-mail: cyprien.lemouchi@ensicaen.fr, loic.le_pluart@ensicaen.fr*

[c] *Normandie Univ, COBRA UMR CNRS 6014,INSA Rouen, UNIROUEN, CNRS, 76000 Rouen, France. Email : muriel.durandetti@univ-rouen.fr*

[d] *Normandie Univ, PBS UMR CNRS 6270, UNIROUEN, 76821 Mont Saint Aignan, France. Email : julie.hardouin@univ-rouen.fr*

[e]*PISSARO Proteomic Facility, IRIB, F-76820 Mont-Saint-Aignan, France*

Contents

1-Materials and Methods

The chemicals were bought from commercial suppliers (Fischer Scientific, Sigma-Aldrich, Strem Chemicals, VWR chemicals, Millipore Sigma and Oakwood Chemicals) and they were used without any further purification. Dried and distillated solvents were used (THF, CH_2Cl_2, $CHCl_3$, triethylamine,…).

The reactions were monitored by Thin layer chromatography (TLC) on Merck Silica gel 60 T254 (coated on aluminium sheet). Column chromatography was performed using silica gel 40-63 µm.

BRUKER Avance III400 and BRUKER Avance III500 were used to record NMR ^{1}H, ^{13}C and ^{31}P spectra in $CDCl_3$ and CH_2Cl_2 using TMS as an internal standard. Chemical shifts are measured in parts per million (ppm). The following notation is used to designate the NMR signals; s: singlet, d: soublet, t: triplet, m: multiplet.

High-resolution ESI-MS (HR-MS). Samples were analyzed by ESI-MS on a high-resolution and high-accuracy mass spectrometer (LTQ-Orbitrap Elite, Thermo Scientific) in positive ion mode. Samples were dissolved in dichloromethane at a concentration between 1 and 5 pmol/µL according to the sample. They were infused at a flow rate of 3 µL/min. The following experimental conditions were applied: spray high voltage, 3 kV; source temperature, 350°C; sheath gas flow rate, 10. External calibration was carried out using the Pierce LTQ Velos ESI positive ion calibration solution. The resolution was set at 240 000 at *m/z* 400.

Gel permeation chromatography (GPC) were performed on the GPC prominence Shimadzu with UV-visible detector SPD-20AV (Double wavelength), A metallooligomers concentration of 1mg/mL were used and the solution were filtered through a 0.45 micron filter before injection. Average molecular weights (Mw, Mn) were determined by GPC against polystyrene standards. THF was used as eluents with a flow rate of 1mL/min.

Attenuated total reflection infrared (ATR IR) spectra were recorded on powders using Spectrum Two from PerkinElmer.

Matrix-assisted laser desorption/ionization time-of-flight mass spectrometry (MALDI-TOF/MS) Experiments were performed by MALDI-TOF/MS (Ultraflex, Bruker Daltonique) in positive ion mode and in reflectron or linear modes. The ion-accelerating voltage was 20 kV. One µL of sample was deposited on the target and was covered with dithranol as the matrix. External calibrations were carried out using the standard protein mixture (Peptide Calibration Standard kit, Bruker Daltonique). At least 150 laser shots were summed for each spectrum. Raw data were processed using Flex Analysis.

Thermogravimetric analysis (TGA) were conducted on Perkin Elmer TGA Pyris 1. The samples were measured into an aluminium pan and sealed before heating with rate of 10 °C/min under a nitrogen atmosphere

The metallooligomers thin films were prepared from solution of the metallooligomers dissolved in CH_2Cl_2 (5mg.mL^{-1}), then they were spin-coated using LabSpin6/8 from SÜSS MicroTec on glass and quartz substrates at 3000 rpm for 100 seconds at 600 rpm.s^{-1} acceleration. The film thicknesses were determined using a KLA-Tencor D-120 stylus profilometer.

UV-Visible absorption. Analysis in CH_2Cl_2 were performed using the Perkin-Elmer (Lambda 35) UV–Vis Spectrometer (250-900 nm) in transmission mode. Room temperature (298 K) film spectra were recorded on a Varian Cary BIO300 spectrophotometer in reflectance mode. 77 K solution spectra were recorded on a Hewlett-Packard 8452A diode array spectrometer for solutions at 77 K in transmission mode. The UV-vis spectra (200 - 900 nm) of film coated quartz substrates were recorded by a Cary 4000 spectrophotometer (Agilent Corporation) in transmission mode using the double-beam mode.

Photoemission analysis. Steady-state measurements, emission and excitation spectra, were made using a Edinburgh Instruments FLS980 Phosphorimeter equipped with single monochromator. Solutions for 298 K measurements were prepared in a glovebox, to avoid excited state quenching by O_2, and sealed in an airtight 1 cm cell. Low temperature measurements were made in an NMR tube using a homemade sample holder. Films were made by spin-coating the polymers on 2.5 cm quartz discs. Measurements exceeding 800 nm were performed using a Photon Technology International QuantaMaster 400 phosphorimeter coupled with a NIR PMT-7-B detector. The fluorescence lifetime measurements were performed on the FLS980 using a 378 nm picosecond pulsed diode laser.

The electrochemical measurements for **P** and **MCzM** were carried out using an BioLogic SP-300 apparatus, at room temperature, under an argon atmosphere, in a three-electrode cell containing anhydrous acetonitrile (MeCN, 10 mL) as solvent and tetrabutylammonium hexafluorophosphate ($TBAPF_6$, 10^{-1} mol.L^{-1}) as supporting salt at a scan rate of 50 mV.s^{-1}. The reference electrode was a saturated Hg/Hg_2Cl_2 reference electrode (further noted SCE for Saturated Calomel Electrode) from Radiometer. It was separated from the cell solution by a bridge compartment filled with the same solvent / supporting electrolyte solution as used in the cell. The counter electrode was a platinum wire. The working electrode was a disk obtained from a cross-section of a platinum wire sealed in Teflon.

Metallooligomers thin films were cast from dichloromethane solution on a platinum disc working electrode (d = 5 mm), **MCzM** solution is prepared in dichloromethane and the cyclic voltammograms were recorded in CH_2Cl_2 solution containing $TBAPF_6$, 10^{-1} mol.L^{-1} as supporting salt at a scan rate of 50 mV.s^{-1}, on a platinum disc working electrode (d = 1 mm).

2-The Ligand L synthesis and characterizations

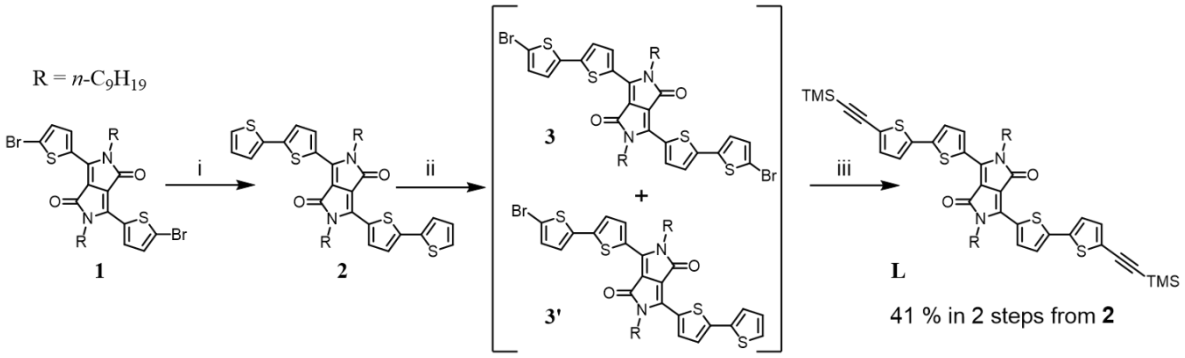

Scheme S1: Synthetic Scheme for **L**. (i) 2-(tributylstannyl)thiophene (2.5 eq.) , $Pd(PPh_3)_2Cl_2$ (10 mol%), PPh_3 (20 mol%), toluene, reflux, overnight, *60 % yield*. (ii) Br_2 (2 eq.), T < 0°C, $CHCl_3$, 3 hrs. (iii) TMSA, $Pd(PPh_3)_2Cl_2$, CuI, THF/iPr_2NH, 70°C, 3hrs.

The intermediate **1** was synthesized according to the procedure reported in our previous work, Nos, M.; Marineau-Plante, G.; Gao, D.; Duranditti, M.; Hardouin, J.; Karsenti, P-L.; Gupta, G.; Sharma, D. G.; Harvey, D. P.; Lemouchi, C.; Le Pluart, L.; *J. Mater. Chem. C*, **2020**, 8, 2363-2380

3,6-di([2,2'-bithiophen]-5-yl)-2,5-dinonyl-2,5-dihydropyrrolo[3,4-c]pyrrole-1,4-dione (2)

The procedure was inspired from the literature, Hongmei Zhan, Qian Liu, Shu-Kong So, Wai-Yeung Wong, *Journal of Organometallic Chemistry* **2019** 894, 1-9**.** In flamed-dried schlenk under argon atmosphere, **1** (170.4 mg, 0.240 mmol) was dissolved in 20 mL of anhydrous and degassed toluene, $Pd(PPh_3)_2Cl_2$ (16.84 mg, 24.0 µmol, 10 mol%) and PPh_3 (12.6 mg, 48.0 µmol, 20 mol%) were added. Then 2-(tributylstannyl)thiophene (commercially available) (227.6 mg, 0.61 mmol, 2.5 eq.) was added. The mixture was refluxed overnight under argon atmosphere, monitored by TLC (R_f=0.6, using pentane/CH_2Cl_2:1/1 as eluent). After cooling, the solvent was evaporated under reduced pressure. The resulting residue was retaken in a mixture CH_2Cl_2/CH_3OH: 30 mL/30 mL, then filtered and washed with methanol several times to get compound **2** as dark-purple solid (104.8 mg, 0.146 mmol, 60 % yield). ^{1}H NMR (500 MHz, $CDCl_3$) δ (ppm):8.90 (d, 2H, *J* = 4.2 Hz), 7.31 (m, 6 H), 7.06 (t, 2H, *J* = 4.2 Hz), 4.07 (t, 4 H, *J* = 7.7 Hz), 1.79-1.72 (m, 4 H), 1.44-1.39 (m, 4 H), 1.36-1.32 (m, 6H), 1.29-1.21 (m, 24H), 0.84 (t, 6H). ^{13}C NMR (500 MHz, $CDCl_3$) δ (ppm): 160.25, 141.81, 138.11, 135.48, 135.15, 127.25, 127.11, 125.29, 124.23, 123.96, 107.16, 41.27, 30.82, 29.00, 28.68, 28.47, 28.22, 25.87, 21.65, 13.08. IR (cm^{-1}): v = 3087 (v, C-H aromatic), 2921 and 2851 (w, v (N-CH_2)), 1657 (w, v(C=O)).

MALDI-tof (dithranol) calc. for $C_{40}H_{48}N_2O_2S_4$ (**2**) [$M^{\cdot+}$], m/z = 716.26; measured [$M^{\cdot+}$]$^+$ m/z = 716.26 ; $T_{m.p.}$ (°C) =233.

3,6-bis(5'-bromo-[2,2'-bithiophen]-5-yl)-2,5-dinonyl-2,5-dihydropyrrolo[3,4-c]pyrrole-1,4-dione (3)

The procedure was inspired from the literature, Catherine Kanimozhi, Nir Yaacobi-Gross, Edmund K. Burnett, Alejandro L. Briseno, Thomas D. Anthopoulos, Ulrike Salznerd, Satish Patil, *Phys. Chem. Chem. Phys.*, **2014**, 16, 17253-17265. In a 50 mL round bottom flask wrapped with aluminum foil to prevent light, **2** (185.0 mg, 0.258 mmol) was dissolved in chloroform (20 mL). The solution was cooled to -5°C with ice bath with NaCl. Keeping the temperature below 0°C, bromine (87 mg, 0.542 mmol) was added. Then, the mixture was stirred at a temperature below 0°C for 3 hours. **Be cautious**: higher temperature causes degradation of the product with by-reactions and provides lower yields. The reaction was monitored by TLC (disappearance of the starting material R_f=0.6 and formation of brominated compound, R_f=0.7, using pentane/CH_2Cl_2:1/1 as eluent). The reaction mixture was quenched with sodium thiosulfate aqueous solution and extracted with methylene chloride. The organic layer was washed twice with water and evaporated under reduced pressure. The liquid residue was retaken several times with toluene and evaporated to remove water traces. The crude product (m = 200 mg) was obtained as a dark purple solid, which is a mixture of **3** and **3'** evidenced by MALDI-TOF. Since the separation of those products was very difficult, the crude material was directly engaged in the next step. **Be cautious**: the brominated compounds are not very stable, they must be stored in the fridge and protected from light exposure, they must be rapidly engaged in the next step. MALDI-TOF (dithranol) calc. for $C_{40}H_{46}Br_2N_2O_2S_4$ (**3**) m/z = 872.08, measured [M+2]$^+$ m/z = 874.10 calc. for $C_{40}H_{47}BrN_2O_2S_4$ (**3'**) m/z = 794.17, measured [M+2]$^+$ m/z = 796.19.

2,5-dinonyl-3,6-bis(5'-((trimethylsilyl)ethynyl)-[2,2'-bithiophen]-5-yl)-2,5 dihydropyrrolo[3,4-c]pyrrole-1,4-dione (L)

The procedure was inspired from the literature, Yuping Yuan, Tsuyoshi Michinobu, Jun Oguma, Takehito Kato, Kunihito Miyake, *Macromol. Chem. Phys.* **2013**, 214, 1465−1472. In flamed-dried Schlenk wrapped with aluminum foil to prevent light and under argon atmosphere, the crude product **3** and **3'** (200 mg) is dissolved in the mixture tetrahydrofuran/ diisopropylamine: 25mL/ 25mL. The solution was degassed with argon stream bubbling into the solution. Then CuI (6.0 mg, 31.5 μmol) and $PdCl_2(PPh_3)_2$ (33.0 mg, 47.0 μmol) were added. Then, trimethylsilylacetylene (TMSA), 98% purity (88.0 mg, 0.896 mmol) was added. The

mixture was heated at 70 °C for 3 hours and monitored by TLC (eluent: CH_2Cl_2/pentane: 40/60, R_f= 0.55). The solution was evaporated under reduced pressure and the crude product was purified by column chromatography on silica gel using pentane/CH_2Cl_2 (60/40) as eluent to provide **L** as a dark blue solid (98 mg, 107.75 µmol, 41 % yield from **2**). ^{1}H NMR (600 MHz,$CDCl_3$) δ (ppm): 8.91 (d, 2H, *J* = 4.2 Hz), 7.30 (d, 2H, *J* = 4.2 Hz), 7.15 (m, 4H), 4.06 (t, 4H, *J* = 7.8 Hz), 1.75 (m, 4H*), 1.44-1.19 (m, 33H*), 0.87 (m, 8H*) *: *nonyl side chains on DPP + supplementary hydrogens from pentane tedious to remove even under strong vacuum*, 0.26 (s, 18H, 2 -Si(CH_3)$_3$). ^{13}C NMR (600 MHz, $CDCl_3$) δ (ppm): 161.23, 142.00, 139.06, 137.41, 136.70, 133.80, 128.73, 125.53, 124.91, 123.98, 108.56, 101.73, 97.10, 42.44, 31.98, 29.63, 29.39, 29.37, 27.03, 22.82, 14.27, 0.07. IR (cm^{-1}): v = 2920 and 2851 (w, v (N-CH_2)), 2140 (w, v(C≡C)), 1659 (w, v(C=O)). HRMS (ESI) Calculated for (**L**) $C_{50}H_{64}N_2O_2S_4Si_2$ [$M^{\cdot+}$]: m/z 908.340. Found: m/z 908.299 ; T $_{m.p}$ (°C) =258.

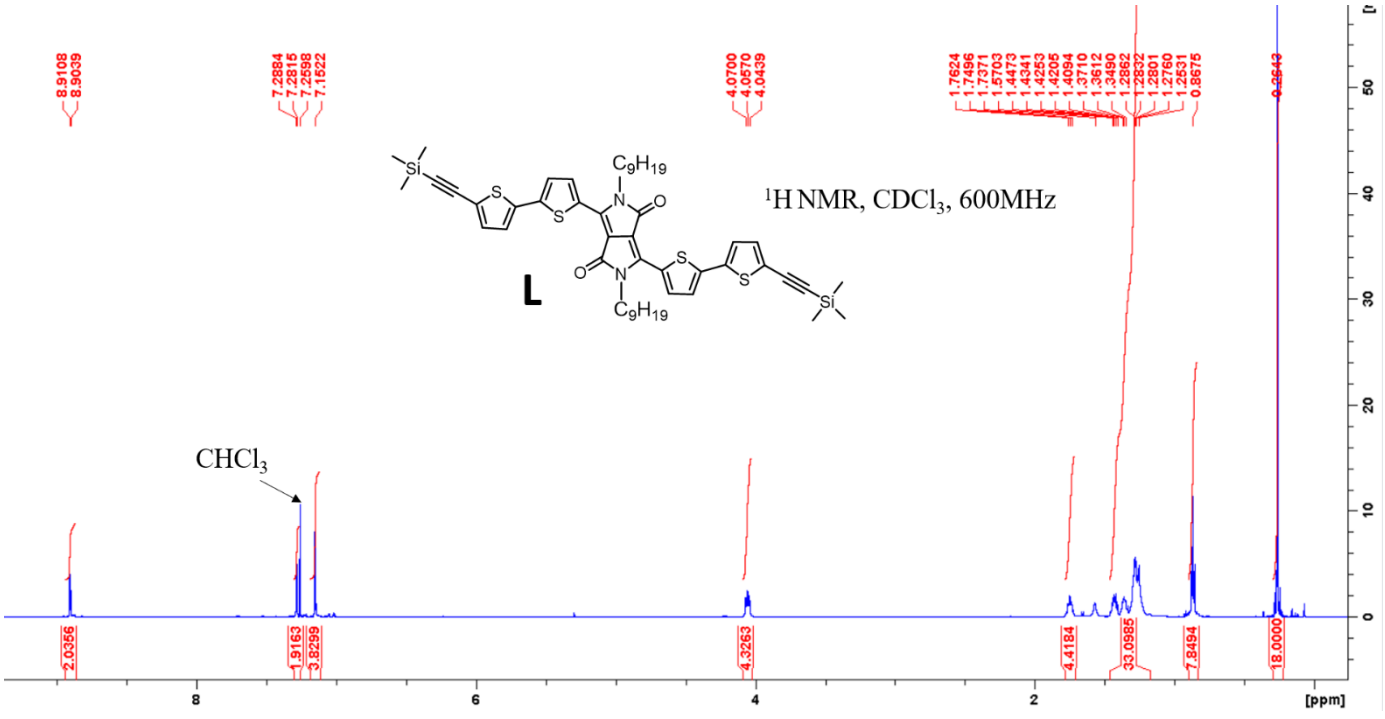

Figure S1: ^{1}H NMR spectra of **L** in $CDCl_3$

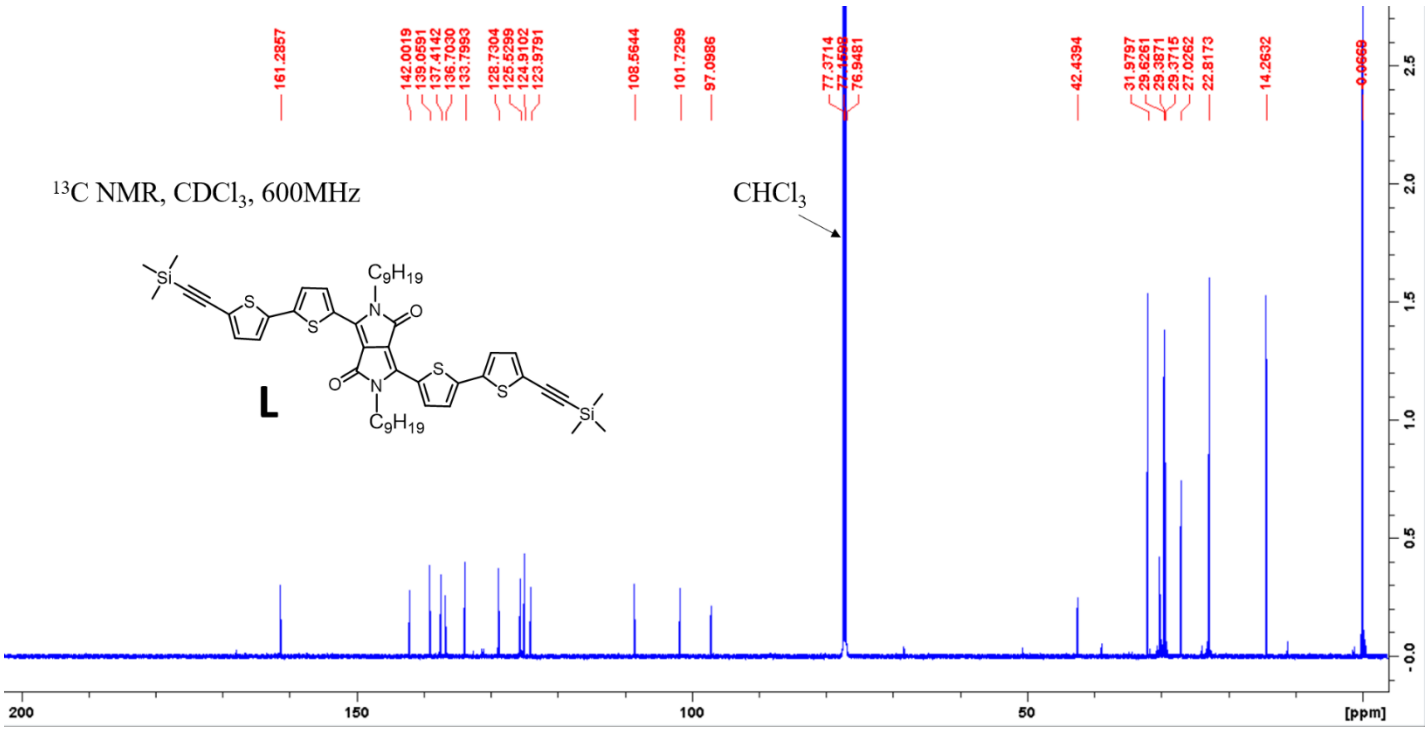

Figure S2: ^{13}C NMR spectra of **L** in $CDCl_3$

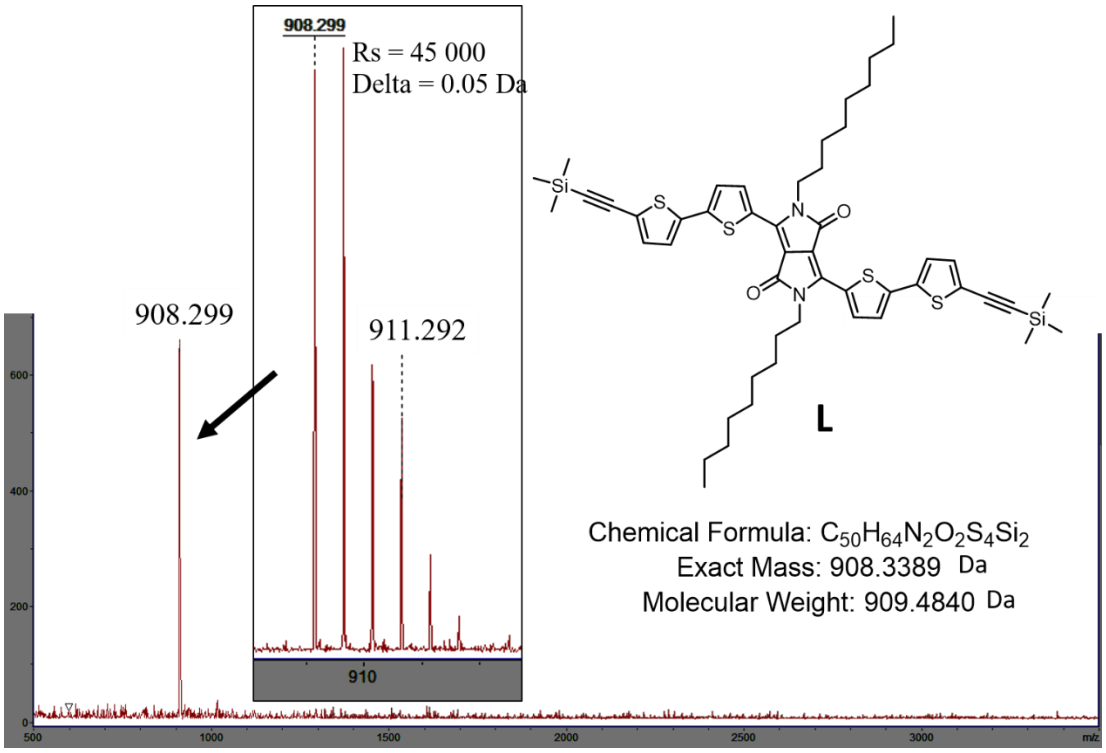

Figure S3: High-resolution ESI-MS (HR-MS) spectrum of **L**, Zoom of molecular peak from $[M^{\cdot+}]$

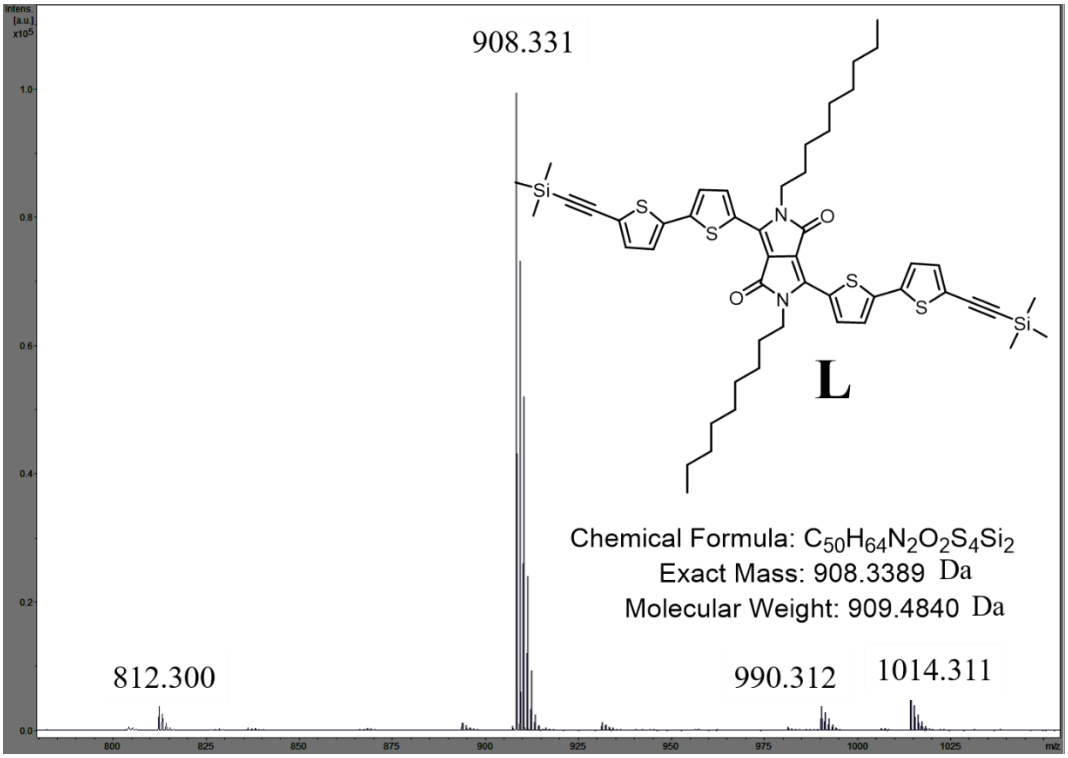

Figure S4: MALDI-TOF/MS spectrum (dithranol matrix) of **L**

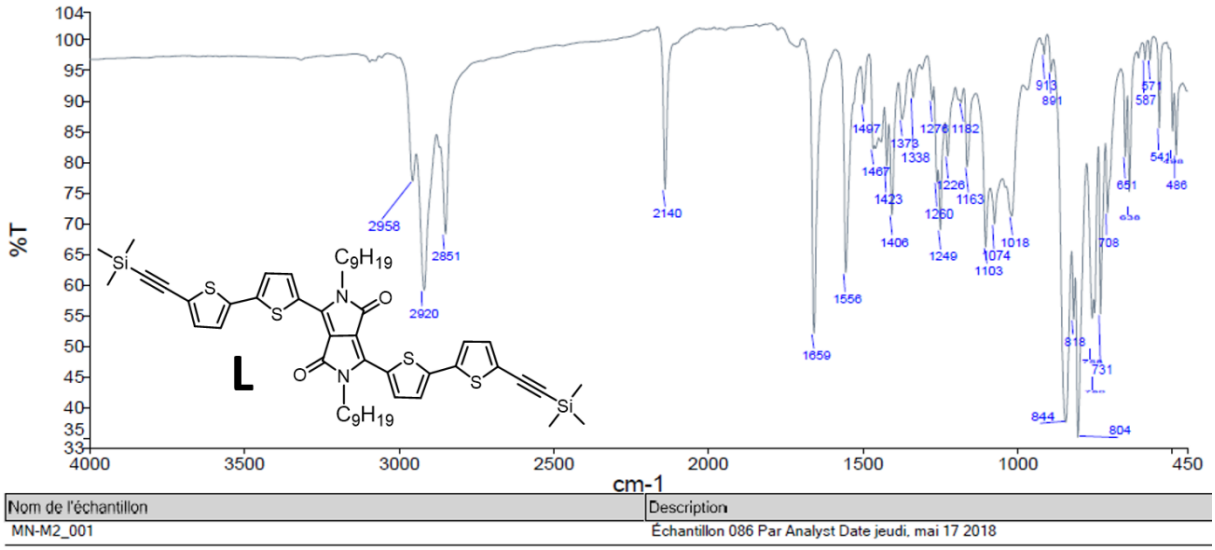

Figure S5: ATR IR spectrum of **L**

3-Optical Properties for the ligand **L**

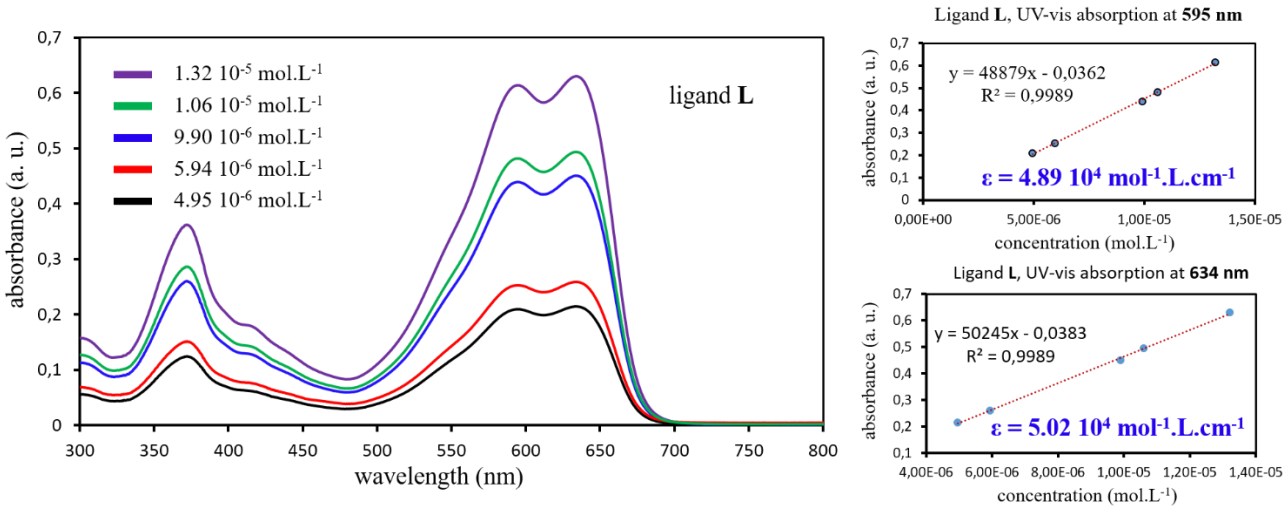

Figure S6: Absorption spectra of the ligand **L** in CH_2Cl_2 at different molar concentrations to calculate the molar extinction coefficient (ε_λ)

4-Metallooligomer synthesis and characterizations

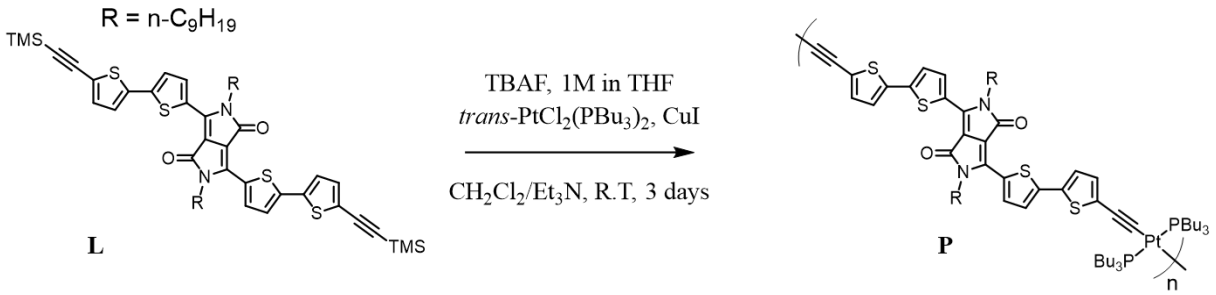

Scheme S2: synthetic route of metallooligomers **P**

Synthesis of short chain metallooligomers P (M_n = 12.4 kg.mol^{-1})

Under argon and dried atmosphere, in a 25 mL flame-dried Schlenk wrapped with aluminum foil, the diethynyl ligand **L** (14 mg, 1 eq., 15.39 µmol) was dissolved in a solvent mixture of freshly distilled and degassed CH_2Cl_2/Et_3N: 4 mL/ 2 mL. The solution was degassed with argon stream bubbling into the solution for 15 minutes. Then copper iodide (0.30 mg, 1.57 µmol, 0.1 eq.) and *trans*-dichlorobis(triethylphosphine)platinum(II) (*trans*-[$PtCl_2$(P*n*-Bu_3)$_2$], (10.3 mg, 1 eq., 15.36 µmol, 1 eq.) were added. Afterwards, tetra-*n*-butylammonium fluoride (TBAF) (33.0 µmol, 2.1 eq., 33 µL of TBAF solution, 1 mol.L^{-1} in THF) was added. The reaction was stirred under argon at room temperature for 3 days. The solution was evaporated under reduced

pressure. The crude material was purified by precipitations in methylene dichloride/methanol (50/50 v/v). In addition, the solid was dissolved in methylene dichloride and purified on Bio Bead X1 ® gel filtration to remove the metallic residues and remaining ligand. The first fraction was collected and evaporated to afford the platinium (II) polyyne oligomers **P** as a dark turquoise colored solid (m=12 mg). ^{1}H-NMR (600 MHz, $CDCl_3$): 8.93 (m, 2H), 7.21 (m, 2H), 7.13 (m, 2H), 6.78 (m, 2H), 4.08 (m, 4H), 2.12 (m, 12H), 1.77-1.24 (m, >40H*), 0.96-0.87 (30 H*) *: *nonyl side chains on DPP + supplementary hydrogens from pentane tedious to remove even under strong vacuum*. ^{31}P-NMR (500 MHz, $CDCl_3$): 3.55 ppm, $^{1}J(^{31}P\text{-}^{195}Pt)$ = 2306 Hz. ATR-IR (cm^{-1}): v = 2919 and 2850 (w, v (N-CH_2)), 2083 (w, v (C≡C)), 1656 and 1657 (w, v(C=O)). T_{dec} = 272, 91 ± 5 °C; GPC (THF): M_n = 12405 $g.mol^{-1}$, M_w= 28283 $g.mol^{-1}$, M_w/M_n = 2.28. The characterizations are in good agreement with reported data for compound analogous to **P**, Yuping Yuan, Tsuyoshi Michinobu, Jun Oguma, Takehito Kato, Kunihito Miyake, *Macromol. Chem. Phys.* **2013**, 214, 1465−1472.

***S*ynthesis of longer chain metallooligomers P'** (M_n = 23.8 $kg.mol^{-1}$)

Under argon and dried atmosphere, in a 25 ml flame-dried Schlenk, the diethynyl ligand **L2** (17 mg, 1.79 eq., 18.70 µmol) was dissolved in a solvent mixture of freshly distilled and degassed CH_2Cl_2/Et_3N: 5 mL/2.5 mL. The solution was degassed with argon stream bubbling into the solution for 15 minutes. Then copper iodide (1 mg, 5.25 µmol, 0.5 eq.) and *trans*-dichlorobis(triethylphosphine)platinum(II) (*trans*-[$PtCl_2$(P*n*-$Bu_3)_2$], (7 mg, 1 eq., 10.44 µmol) were added. Afterwards, tetra-*n*-butylammonium fluoride (40 µmol, 3.83 eq., 40 µL of TBAF 1 $mol.L^{-1}$ in THF) (3.8 eq.) was added. The reaction was stirred at room temperature for 3 days under argon. The solution was evaporated under reduced pressure. The crude material was purified by precipitations in methylene dichloride/methanol (50/50 v/v). In addition, the solid was dissolved in methylene dichloride and purified on Bio Bead X1 ® gel filtration to remove the metallic residues and remaining ligand. The first fraction was collected and evaporated to afford the platinium (II) polyyne oligomers **P'** as a dark turquoise colored solid (m=6 mg). ^{1}H-NMR (600 MHz, $CDCl_3$): 8.93 (m, 2H), 7.21 (m, 2H), 7.13 (m, 2H), 6.78 (m, 2H), 4.08 (m, 4H), 2.12 (m, 12H), 1.77-1.24 (m, >40H*), 0.96-0.87 (30 H*) *: *nonyl side chains on DPP + supplementary hydrogens from pentane tedious to remove even under strong vacuum*. ^{31}P-NMR (500 MHz, $CDCl_3$): 3.55 ppm, $^{1}J(^{31}P\text{-}^{195}Pt)$ = 2306 Hz. ATR-IR (cm^{-1}): v = 2919 and 2850 (w, v (N-CH_2)), 2083 (w, v (C≡C)), 1656 and 1657 (w, v(C=O)). T_{dec} = 272, 91 ± 5 °C; GPC (THF): M_n = 23811 $g.mol^{-1}$, M_w= 63845 $g.mol^{-1}$, M_w/M_n = 2.77. The characterizations are in good agreement with reported data for compound analogous to **P'**, Yuping Yuan, Tsuyoshi

Michinobu, Jun Oguma, Takehito Kato, Kunihito Miyake, *Macromol. Chem. Phys.* **2013**, 214, 1465−1472.

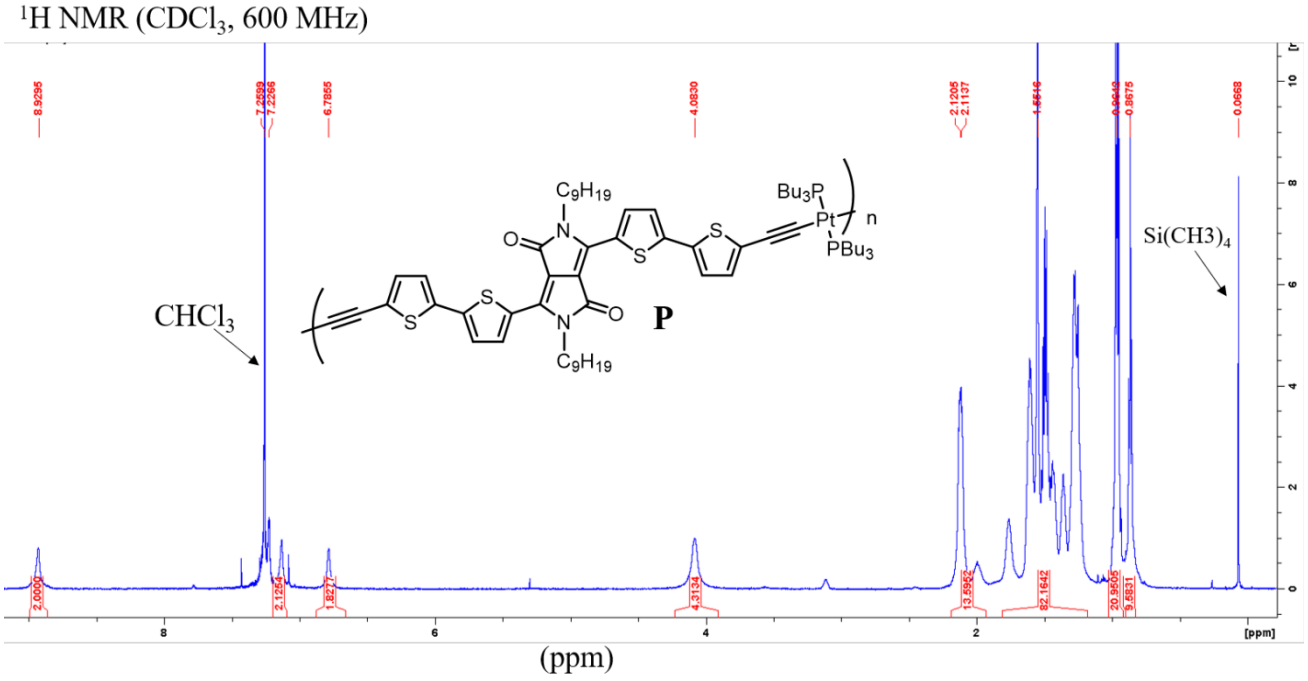

Figure S7: ^{1}H NMR spectra of **P** in $CDCl_3$

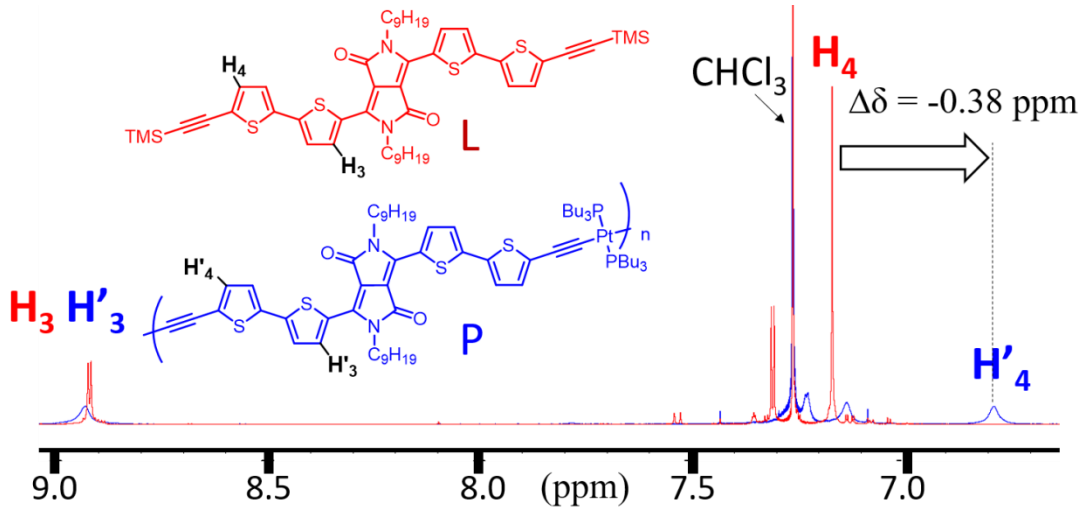

Figure S8: ^{1}H NMR (600 MHz, $CDCl_3$), proton chemical shift comparison between ligand **L** and metallooligomer **P** in $CDCl_3$

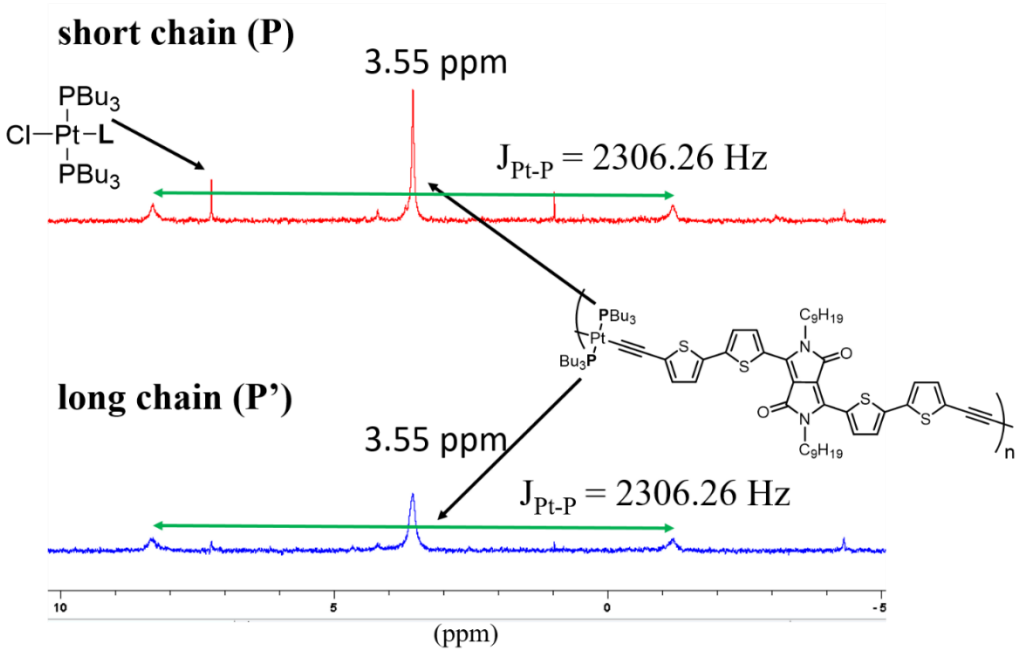

Figure S9: $^{31}P\{1H\}$ NMR spectra of **P** (short chain) and **P'** (long chain) in $CDCl_3$

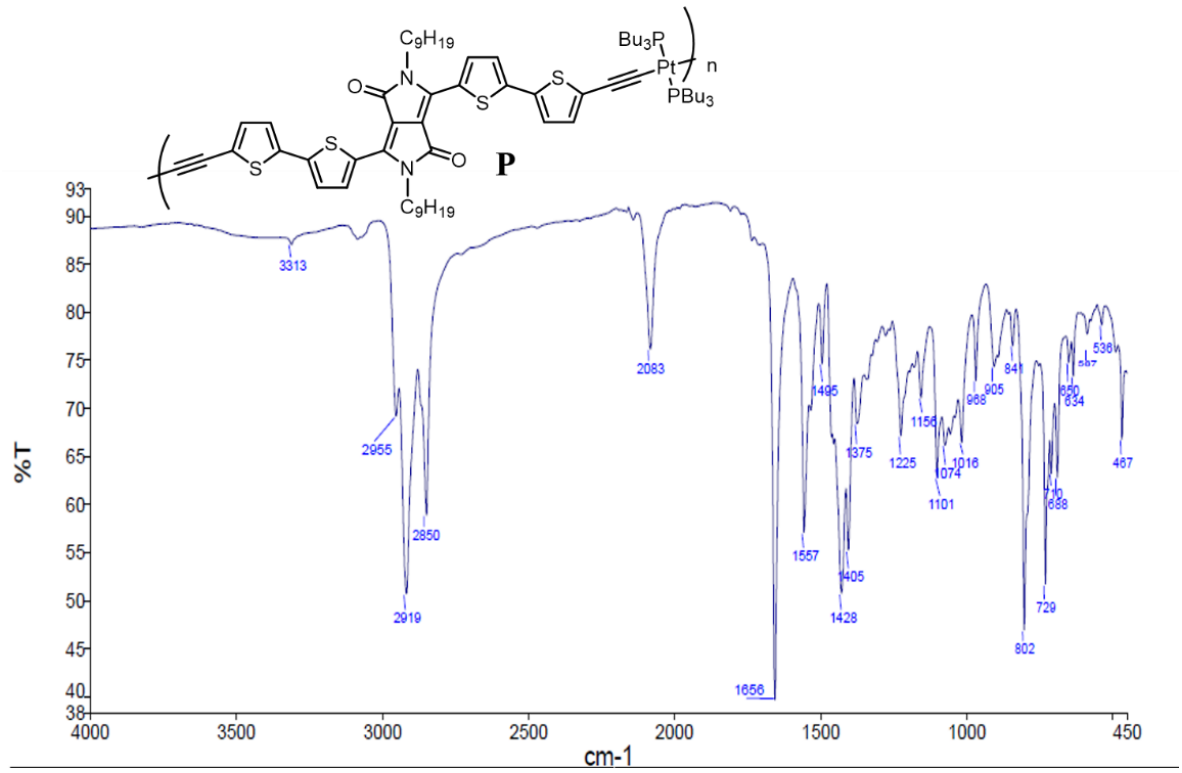

Figure S10: ATR IR spectrum of **P**

5. GPC analysis

Number- and weight-average molar mass (M_n and M_w respectively) were determined by gel permeation chromatography (GPC) against polystyrene standards in THF with a flow rate of 1 mL/min

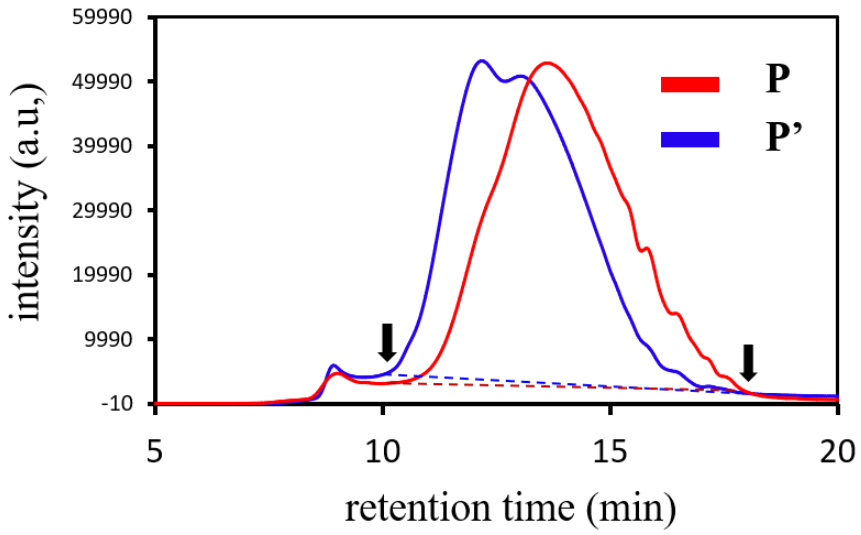

Figure S11: GPC chromatograms of the metallooligomers **P** (short chains) and **P'** (long chains)

	M_n (g.mol^{-1})	M_w (g.mol^{-1})	M_w/M_n	Number Repeat units
P	12405	28283	2.28	9-10
P	12-13 kg mol^{-1}		2-2.5	9-10
P'	23811	63845	2.77	17-18
P'	23-24 kg mol^{-1}		2.5-3	17-18

Be cautious: a discoloration of the **P** and **P'** solution in THF from greenish to light yellowish was observed after 1 hour, which evidences a decomposition of the metallooligomers.

6 MALDI-TOF of the metallooligomers P

The analysis of the metallooligomers **P** by matrix-assisted laser desorption/ionization time-of-flight mass spectrometry (MALDI-TOF/MS) were performed with the 2-[(2E)-3-(4-tert-Butylphenyl)-2-methylprop-2-enylidene]malononitrile (DCTB) matrix, in solution with a concentration of 10 mg mL^{-1} in methylene dichloride following the literature procedure[1].

[1] (a) M. F. Wyatt,B. K. Stein, A. G. Brenton, *Anal. Chem*. **2006,** 78, 199. (b) J. Mei, K. Ogawa, Y.-G. Kim, N. C. Heston, D. J. Arenas, Z. Nasrollahi, T. D. McCarley, D. B. Tanner, J. R. Reynolds, K. S. Schanze, *Applied Mat Interfaces*, **2009**, 1,150.

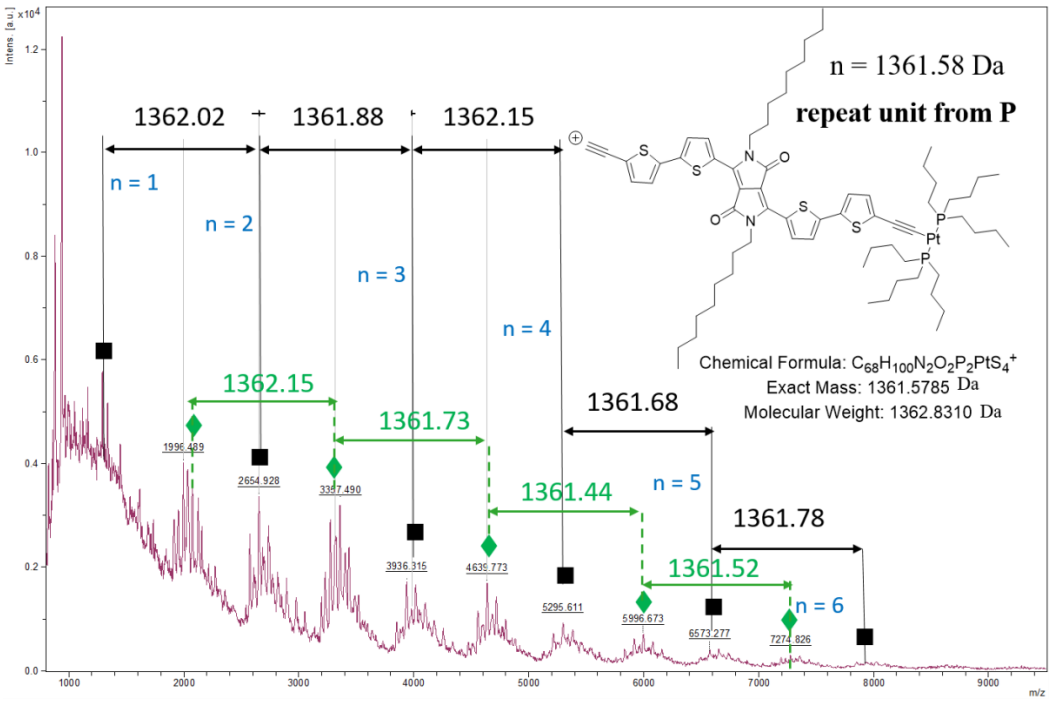

Figure S12: MALDI-TOF/MS spectra of **P** with

7. Thermogravimetric analysis (TGA)

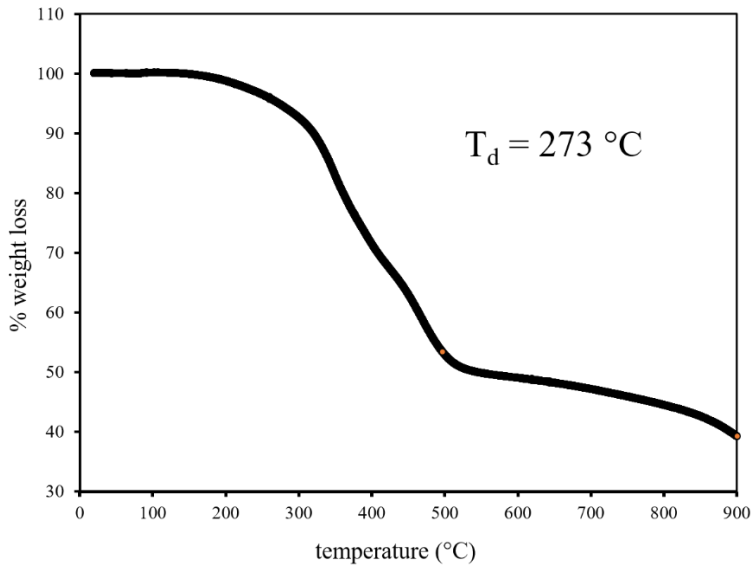

Figure S13: Thermogravimetric analysis (TGA) of **P** measuring at a heating rate of 10°C.min^{-1} under a 80 mL/min N_2(g) flow. a: the decomposition onset was defined by a 5 wt% loss.

8- Electrochemical characterization

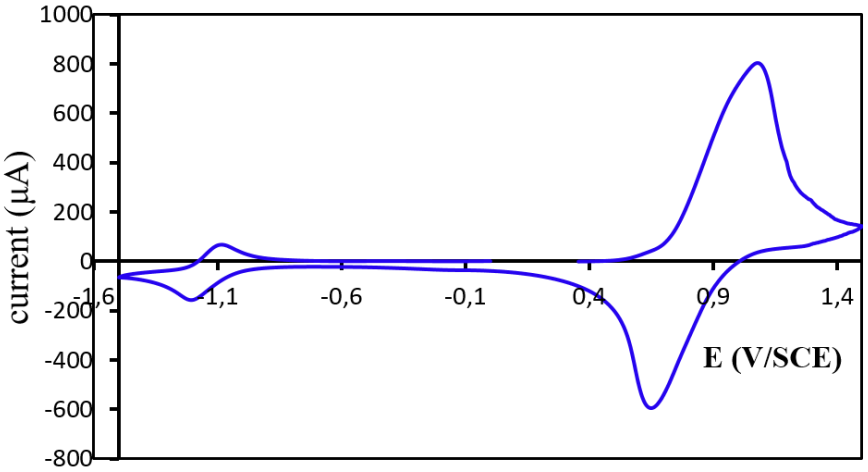

Figure S15: CVs of the **P** metallooligomers. The oligomers thin films were cast from a CH_2Cl_2 solution onto a platinum disc working electrode (d = 5 mm), and the CVs were recorded in CH_3CN solution containing NBu_4PF_6, 10^{-1} mol.L^{-1} as supporting electrolyte (scan rate of 50 mV.s^{-1}).

	$E_{onset(ox)}$ V/ECS	$E_{onset(red)}$ V/ECS	HOMO eV	LUMO eV	$E_g^{elec.}$ eV
P	0.71	-1.00	-5.44	-3.73	1.71

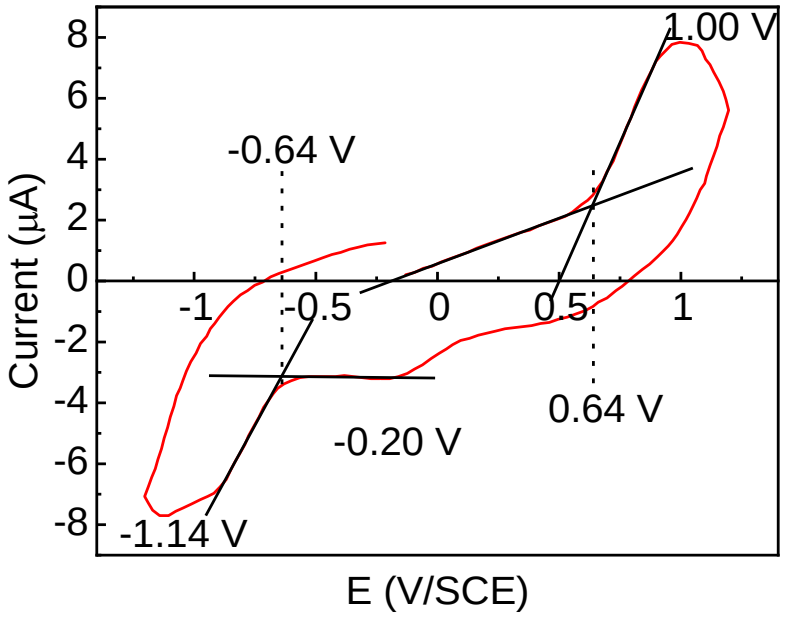

Figure S16: CVs of the **MCzM** (c = $1.2 \cdot 10^{-4}$ mol.L^{-1}) in CH_2Cl_2 on a platinum disc working electrode (d = 1 mm), and the CVs were recorded in solution containing NBu_4PF_6, 10^{-1} mol.L^{-1} as supporting electrolyte (scan rate of 50 mV.s^{-1}).

	$E_{onset(ox)}$ V/ECS	$E_{onset(red)}$ V/ECS	HOMO eV	LUMO eV	$E_g^{elec.}$ eV
MCzM	0.64	-0.64	-5.37	-4.09	1.28

9- DFT and TDDFT computations.

Computations. The density functional theory (DFT) and time dependent density functional theory (TDDFT) calculations were performed with Gaussian 16[1] at the Université de Sherbrooke with the Mammouth supercomputer supported by *Le Réseau Québécois De Calculs Hautes Performances*. The neutral 1D-polymer was drawn and extended by 4.5 motifs and used as a starting point for the calculations. The cationic and anionic form were obtained after adjusting the charge of the previously optimized neutral form. The DFT (ground states) as well as TDDFT calculations[2–10] were carried out using the PBE0 method. The 6-31g* basis set was used for C, H, N, P, S and O.[10] VDZ (valence double ζ) with SBKJC effective core potentials was used for all Pt atoms.[11] All calculations were carried out with a dichloromethane cpcm solvent field. No imaginary frequencies were observed validating the correct energy minimization after the optimization. The calculated absorption spectra were obtained from GaussSum 3.0.[12] Isosurface were generated with a isovalue of 0.02, red lobes are positive and green lobes are negative.

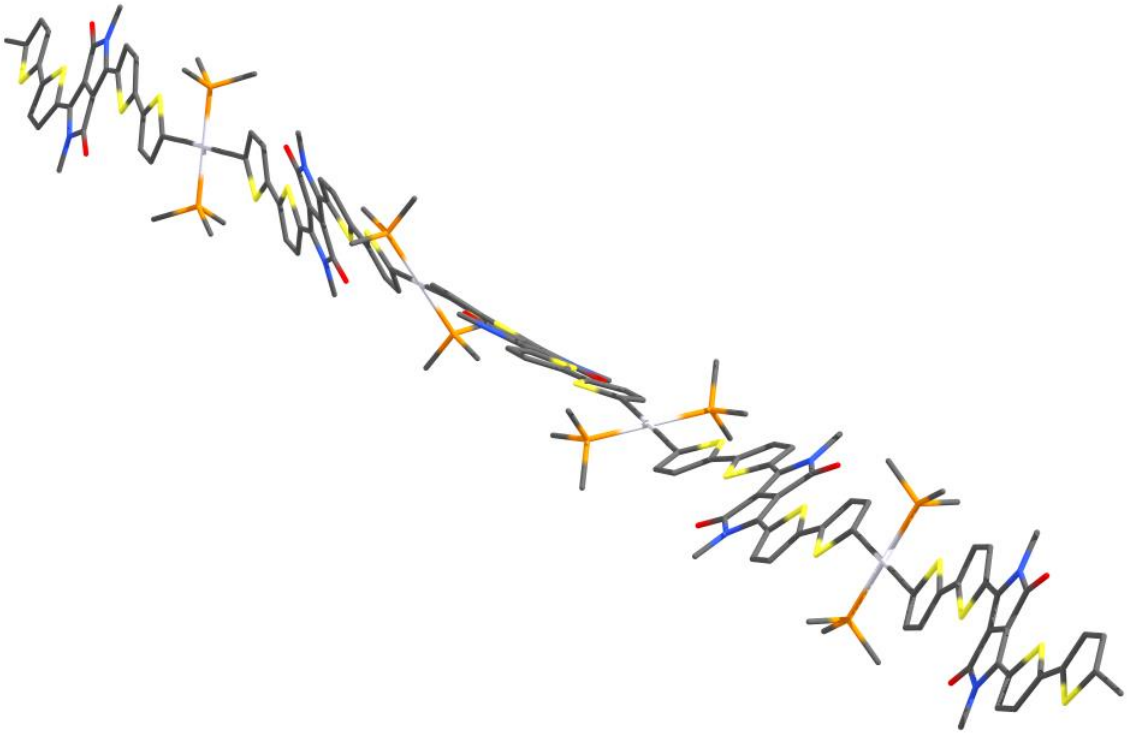

Figure S17: Optimized structure of **P** showing the twisting effect along the length of the oligomer.

HOMO -4 (-5.126)

HOMO -3 (-5.107)

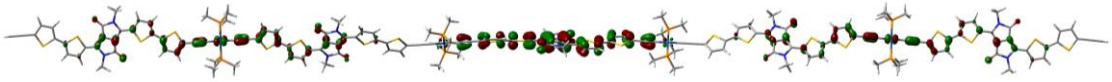

HOMO -2 (-5.018)

HOMO -1 (-4.952)

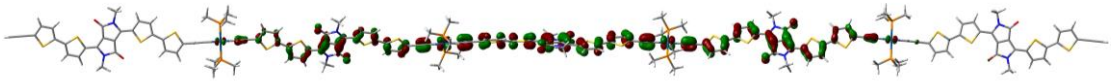

HOMO (-4.912)

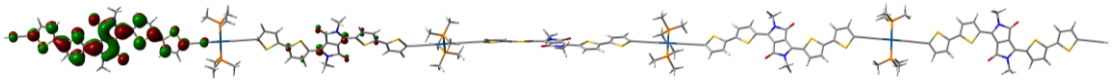

LUMO (-2.815)

LUMO +1 (-2.811)

LUMO +2 (-2.756)

LUMO +3 (-2.729)

LUMO +4 (-2.698)

Figure S18: Representations of the frontier MOs for **P**. (MOs= molecular orbitals). E_{tot} = -511471.4941 eV

Table S1: Relative atomic contributions (%) of the various fragments to the frontier MOs of **P**.

Fragments	H-4	H-3	H-2	H-1	HOMO	LUMO	L+1	L+2	L+3	L+4
Ethynyl	5.8	8.9	9.9	11.3	11.9	5.2	2.7	2.6	2.5	2.2
DPP	**46.6**	41.0	36.4	32.8	31.2	43.4	43.6	43.8	44.6	45.5
Thiophene	46.3	**46.7**	**48.7**	**49.6**	**50.1**	**50.7**	**53.1**	**52.4**	**51.8**	**51.2**
Phosphine	0.2	0.2	0.4	0.3	0.4	0.3	0.3	0.5	0.3	0.2
Platinum	1.1	3.2	4.6	6.0	6.5	0.4	0.4	0.7	0.8	0.9

Table S2: Calculated position, oscillator strength (f) and major contributions of the first 100 singlet-singlet electronic transitions for **P**.

Wavelength (nm)	Osc, Strength	Major contributions
719.9	10.2295	H-1→L+3 (17%), HOMO→L+2 (40%)
705.1	0.0809	H-1→LUMO (13%), H-1→L+2 (12%), HOMO→L+3 (20%)
683.1	0.629	HOMO→L+2 (15%), HOMO→L+4 (16%)
664.7	0.0108	H-4→L+1 (10%), H-3→LUMO (15%), H-1→L+2 (15%), HOMO→L+3 (18%)
658.1	0.3135	H-2→L+2 (15%), H-1→L+3 (23%), HOMO→L+4 (27%)
614.3	0.1163	H-3→LUMO (12%), HOMO→LUMO (61%)
613.4	0.1933	HOMO→L+1 (61%)
603.1	0.0028	H-1→LUMO (17%), H-1→L+2 (21%), HOMO→L+3 (26%)
600.0	0.0245	H-1→LUMO (22%), H-1→L+1 (19%), HOMO→LUMO (11%), HOMO→L+4 (13%)
597.2	0.0014	H-1→L+1 (15%), H-1→L+2 (25%), H-1→L+4 (21%)
593.7	0	H-2→L+2 (31%), HOMO→L+4 (28%)
592.3	0.0019	H-2→L+3 (28%), H-1→L+1 (12%), H-1→L+4 (17%), HOMO→L+3 (17%)
588.3	0.1408	H-2→L+2 (11%), H-2→L+4 (24%), H-1→L+3 (18%), HOMO→L+2 (34%)
578.5	0.0016	H-2→LUMO (61%)
577.3	0.0017	H-4→L+1 (10%), H-2→L+1 (58%)
571.9	0.0052	H-4→L+3 (11%), H-3→L+2 (18%), H-2→L+3 (27%), H-1→L+4 (13%), HOMO→L+3 (12%)
570.9	0.0229	H-4→L+2 (17%), H-3→L+3 (27%), H-2→L+4 (23%)

564.4	0.0097	H-4→L+3 (23%), H-3→L+2 (22%), H-2→L+3 (22%), H-1→L+2 (11%)
562.8	0.1033	H-4→L+2 (16%), H-4→L+4 (11%), H-3→L+3 (16%), H-2→L+4 (23%), H-1→L+3 (20%)
548.4	0.0001	H-4→LUMO (11%), H-4→L+1 (32%), H-3→LUMO (12%), H-3→L+1 (33%)
548.2	0.0016	H-4→LUMO (47%), H-3→LUMO (22%), H-3→L+1 (17%)
543.9	0.0025	H-4→L+3 (13%), H-3→L+2 (33%), H-3→L+4 (31%)
541.1	0.0046	H-4→L+2 (52%), H-4→L+4 (17%), H-3→L+3 (15%)
530.5	0.0001	H-4→L+3 (39%), H-3→L+4 (44%)
529.2	0.0042	H-4→L+4 (59%), H-3→L+3 (25%)
524.7	0.0021	H-5→LUMO (10%), H-5→L+2 (42%)
520.4	0.0008	H-6→LUMO (15%), H-5→LUMO (13%), H-5→L+1 (18%), H-5→L+3 (16%)
515.0	0.0307	H-6→L+1 (13%), H-5→LUMO (10%), H-5→L+2 (21%), H-5→L+4 (10%)
508.6	0.0081	H-6→L+2 (16%), H-5→L+3 (39%)
505.1	0.0101	H-6→L+3 (20%), H-5→L+4 (50%)
488.5	0.0115	H-6→LUMO (15%), H-6→L+2 (10%), H-5→LUMO (34%), H-5→L+1 (11%)
487.7	0.0171	H-7→L+1 (10%), H-6→L+1 (15%), H-5→LUMO (15%), H-5→L+1 (32%)
484.0	0.0693	H-6→L+2 (35%), H-6→L+4 (22%)
478.4	0.0281	H-7→L+2 (16%), H-7→L+4 (10%), H-6→L+3 (20%), H-5→L+4 (11%)
478.1	0.1173	H-8→L+2 (11%), H-7→L+3 (26%), H-6→L+4 (17%)
468.8	0.0132	H-7→LUMO (17%), H-6→LUMO (19%), H-6→L+1 (10%)
468.0	0.0081	H-6→LUMO (12%), HOMO→L+5 (17%)
467.6	0.003	H-7→L+1 (13%), H-6→L+1 (18%), HOMO→L+5 (13%)
464.8	0.1359	H-2→L+6 (10%), H-1→L+5 (28%), HOMO→L+6 (15%)
462.1	0.0032	H-8→L+3 (11%), H-7→L+2 (21%), H-6→L+3 (23%)
459.9	0.0092	H-7→L+3 (13%), H-6→L+4 (23%)
459.1	0.0162	H-7→L+2 (15%), H-7→L+4 (18%), H-2→L+5 (10%)

453.3	0.0007	H-7→L+4 (18%), HOMO→L+7 (12%)
450.7	0.0289	H-8→L+2 (14%)
449.1	0.2198	H-8→L+2 (19%), H-8→L+4 (15%)
446.8	0.0105	H-8→LUMO (11%), H-8→L+1 (12%), H-7→LUMO (11%), H-7→L+4 (12%)
443.7	0.1395	H-8→LUMO (27%), H-8→L+1 (14%)
441.8	0.0083	H-8→L+1 (23%), H-4→L+5 (10%), H-2→L+7 (12%), H-1→L+8 (10%), HOMO→L+9 (10%)
439.0	0.0017	H-8→L+3 (22%), H-7→L+3 (12%), H-7→L+4 (16%)
438.1	0.0005	H-8→L+3 (12%), H-8→L+4 (17%), H-7→L+3 (17%)
428.6	0.0611	H-10→LUMO (20%), H-9→LUMO (32%), H-8→LUMO (16%)
427.3	0.0311	H-10→L+1 (24%), H-9→L+1 (28%), H-8→L+1 (14%)
425.1	0.0002	H-9→L+2 (52%), H-8→L+3 (10%)
422.1	0.0074	H-1→L+7 (16%), HOMO→L+6 (48%)
420.9	0.0263	H-10→L+2 (17%), H-9→L+3 (27%), HOMO→L+6 (10%)
420.6	0.0002	HOMO→L+5 (34%), HOMO→L+7 (22%)
418.8	0.0098	H-10→L+2 (13%)
418.1	0.0071	H-11→L+2 (16%), H-10→L+3 (22%), H-9→L+4 (13%)
417.2	0.2439	H-11→L+3 (19%), H-9→L+4 (10%)
416.6	0.084	H-12→L+2 (17%), H-10→L+4 (19%), H-9→L+3 (10%)
415.8	0.0486	H-9→L+4 (13%), H-1→L+6 (13%), HOMO→L+5 (13%)
415.2	0.037	H-9→L+4 (18%), H-1→L+6 (18%)
414.0	0.0092	H-13→LUMO (17%), H-3→L+5 (12%), H-1→L+5 (21%), HOMO→L+8 (15%)
413.7	0.0225	H-14→L+1 (20%), H-13→LUMO (15%), H-1→L+6 (14%)
411.7	0.7052	H-14→L+1 (16%), H-1→L+9 (13%)
409.6	0.0034	H-4→L+5 (10%), H-2→L+5 (27%), H-1→L+8 (10%), HOMO→L+9 (28%)
408.9	0.1051	H-2→L+8 (11%), H-1→L+5 (12%), H-1→L+7 (28%), HOMO→L+6 (14%), HOMO→L+8 (17%)
406.8	0.0448	H-11→LUMO (10%), H-10→LUMO (26%), H-9→LUMO (38%)
406.6	0.0635	H-10→L+1 (25%), H-9→L+1 (42%)

404.3	0.0234	H-2→L+5 (10%), H-2→L+7 (12%), H-2→L+9 (20%), H-1→L+6 (13%), H-1→L+8 (13%), HOMO→L+7 (13%)
403.3	0.4869	H-3→L+5 (12%), H-2→L+6 (34%)
401.4	0.0136	H-3→L+8 (11%), H-2→L+7 (28%), HOMO→L+9 (10%)
399.4	0.0352	H-4→L+7 (16%), H-3→L+8 (13%), H-1→L+8 (11%), HOMO→L+7 (11%), HOMO→L+9 (25%)
397.7	0.1154	H-4→L+8 (20%), H-3→L+7 (19%), H-2→L+6 (10%), H-1→L+9 (12%), HOMO→L+8 (10%)
397.2	0.0019	H-11→LUMO (17%), H-10→LUMO (13%), H-10→L+3 (22%)
396.9	0.0014	H-11→LUMO (15%), H-11→L+1 (11%), H-10→LUMO (20%), H-10→L+4 (10%), H-9→L+3 (12%)
393.0	0.0004	H-12→L+3 (10%), H-11→L+1 (10%), H-11→L+2 (12%), H-10→L+1 (11%), H-10→L+3 (30%)
392.6	0.0202	H-12→L+4 (10%), H-11→L+1 (15%), H-10→L+2 (18%), H-10→L+4 (17%), H-9→L+3 (10%)
391.7	0.0162	H-2→L+8 (43%), H-1→L+7 (10%), H-1→L+9 (27%)
391.0	0.0094	H-4→L+5 (36%), H-3→L+6 (31%)
390.0	0.0078	H-4→L+6 (43%), H-3→L+5 (35%)
389.6	0.0083	H-12→L+2 (13%), H-11→L+2 (20%), H-11→L+4 (12%), H-10→L+2 (12%), H-10→L+4 (12%)
388.7	0.0001	H-4→L+9 (10%), H-2→L+9 (28%), H-1→L+8 (15%)
388.5	0.0052	H-12→L+2 (15%), H-11→L+2 (18%), H-11→L+4 (15%), H-10→L+4 (10%)
386.3	0.0002	H-12→L+1 (56%), H-11→L+1 (25%)
385.7	0.0001	H-12→LUMO (69%), H-11→LUMO (13%)
385.2	0.1068	H-5→L+7 (14%), H-4→L+8 (10%), H-3→L+7 (12%), H-1→L+9 (10%)
383.7	1.1742	H-5→L+5 (13%), H-3→L+7 (26%), HOMO→L+10 (14%)
383.3	0.0339	H-4→L+7 (46%)
380.5	0.0148	H-6→L+5 (10%), H-5→L+6 (10%), H-3→L+8 (16%), H-2→L+9 (11%)
379.8	0.0015	H-12→L+3 (18%), H-12→L+4 (11%), H-11→L+3 (22%), H-11→L+4 (23%)
379.3	0.0042	H-15→L+1 (68%)

378.7	0.0028	H-12→L+3 (27%), H-12→L+4 (13%), H-11→L+3 (15%), H-11→L+4 (11%)
378.0	0.0527	H-12→L+4 (14%), H-5→L+5 (12%), HOMO→L+10 (21%)
377.4	0.0071	H-16→LUMO (56%)
377.0	0.0113	H-35→L+1 (12%), H-34→LUMO (48%)
376.7	0.0082	H-35→L+1 (37%), H-4→L+8 (11%)
375.6	0.0341	H-1→L+10 (11%)
375.3	0.0567	H-35→L+1 (15%), H-34→LUMO (10%), H-4→L+8 (19%)
374.6	0.0014	H-35→L+1 (8%), H-34→LUMO (6%), H-33→L+2 (6%), H-33→L+3 (7%), H-33→L+4 (3%), H-32→L+2 (3%), H-32→L+3 (6%), H-31→L+4 (6%), H-7→L+6 (4%), H-6→L+5 (5%), H-5→L+6 (6%), H-3→L+8 (6%), H-1→L+10 (4%), HOMO→L+11 (2%)

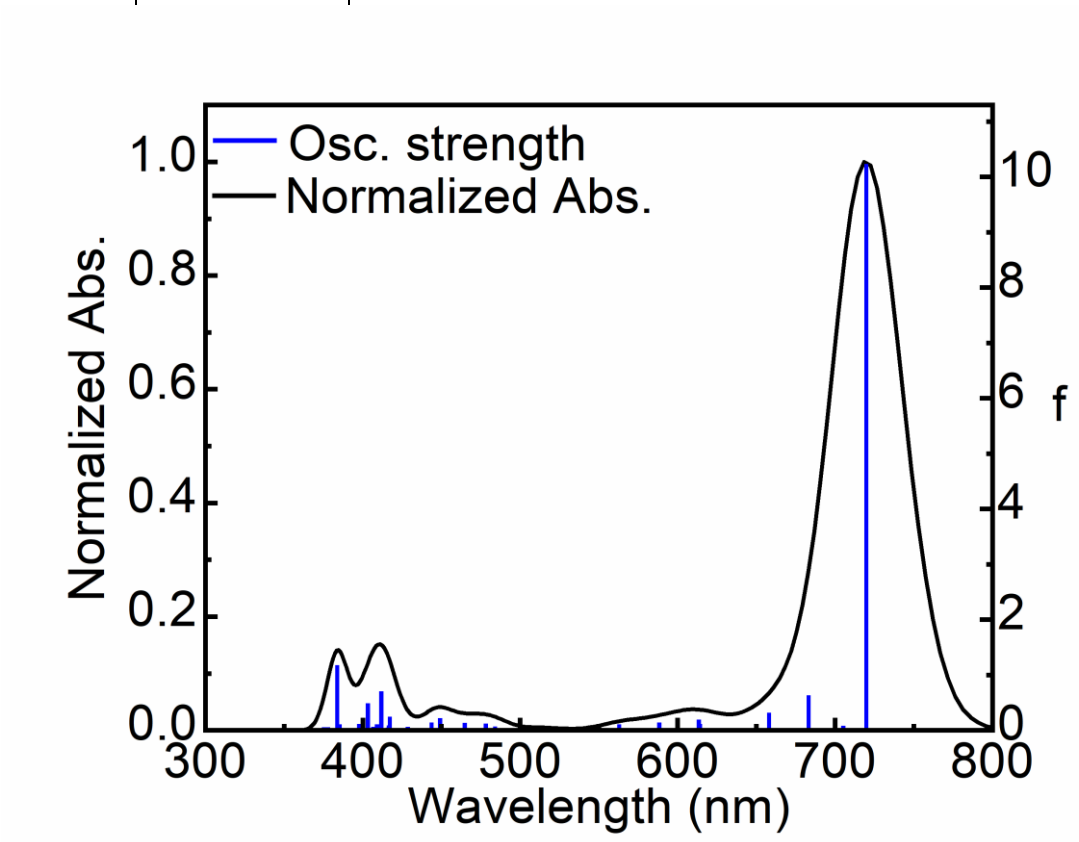

Figure S19: Bar graph reporting the calculated oscillator strength and calculated position of the electronic transitions calculated by TDDFT for **P** (bar graph; f = computed oscillator strength).

10- The fluorescence decays

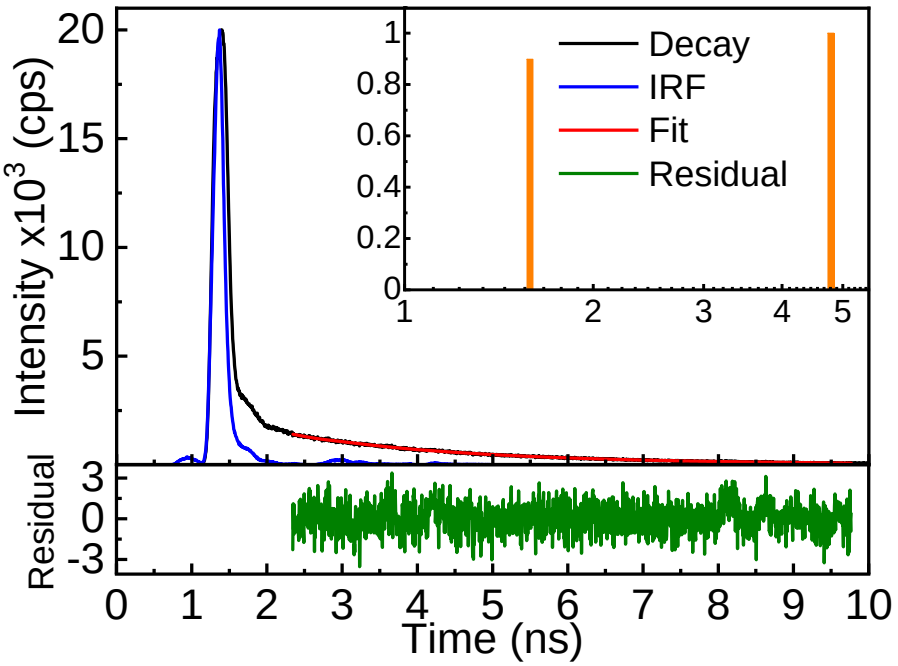

Figure S20: Emission decay (black) of MCzD in solution in DCM at 298K, residuals (green), IRF (blue) and best fit (red). Multi-exponential analysis yields τ_P = 1.585 ns (47.3%), 4.788 ns (52.7%), χ^2 = 1.079. Inset, Multi-exponential analysis. λ_{ex}= 477 nm, λ_{em} = 604 nm.

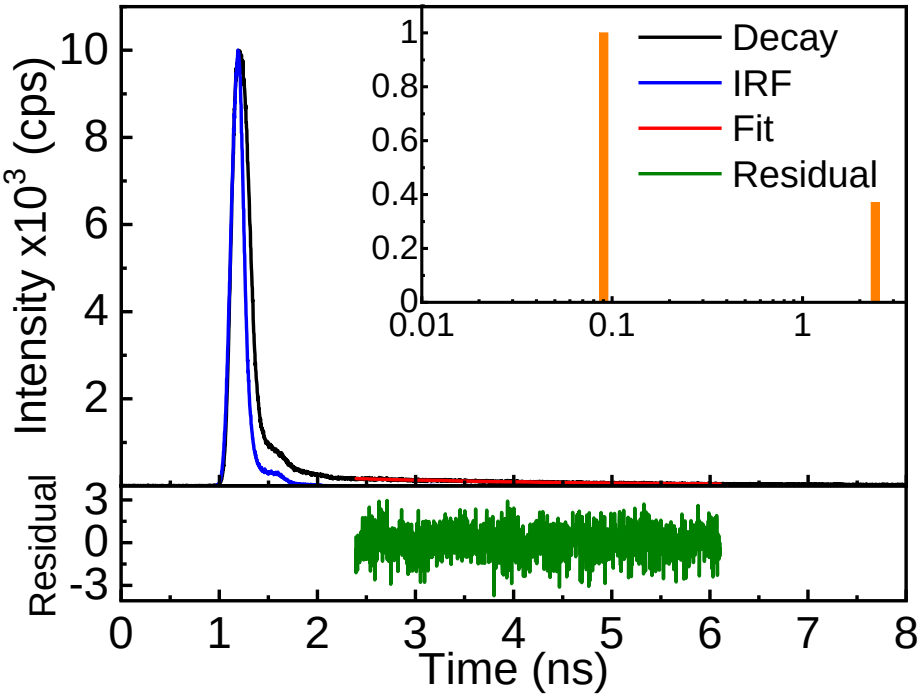

Figure S21: Emission decay (black) of MCzM in solution in DCM at 298K, residuals (green), IRF (blue) and best fit (red). Multi-exponential analysis yields τ_P = 0.090 ns (72.9%), 2.412 ns (27.1%), χ^2 = 1.057. Inset, Multi-exponential analysis. λ_{ex}= 477 nm, λ_{em} = 607 nm.

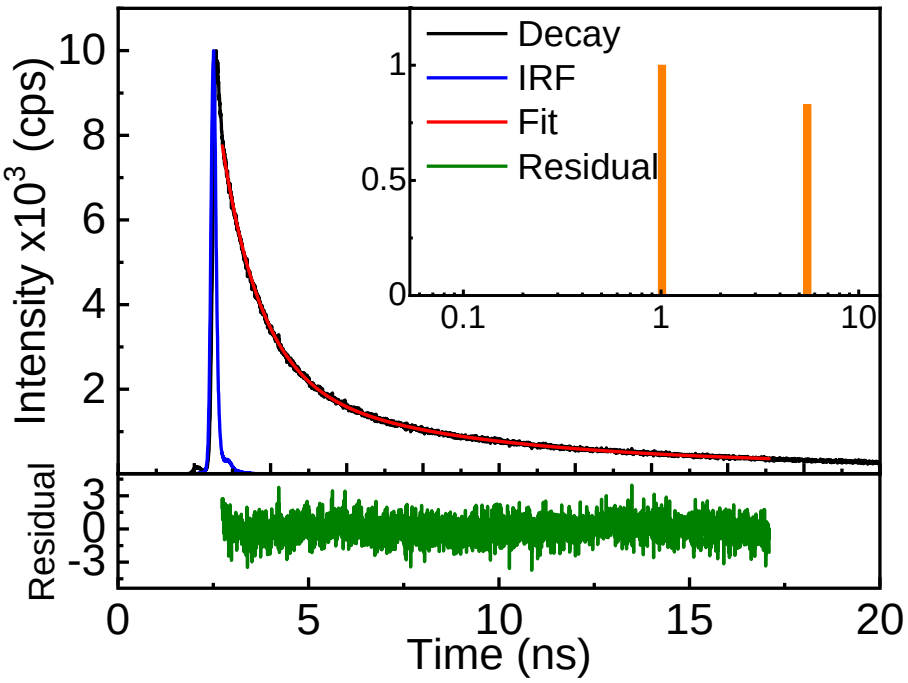

Figure S22: Emission decay (black) of $PC_{61}BM$ in solution in DCM at 298K, residuals (green), IRF (blue) and best fit (red). Multi-exponential analysis yields τ_P = 1.011 ns (54.7%), 5.496 ns (45.3%), χ^2 = 1.005. Inset, Multi-exponential analysis. λ_{ex}= 378 nm, λ_{em} = 465 nm.

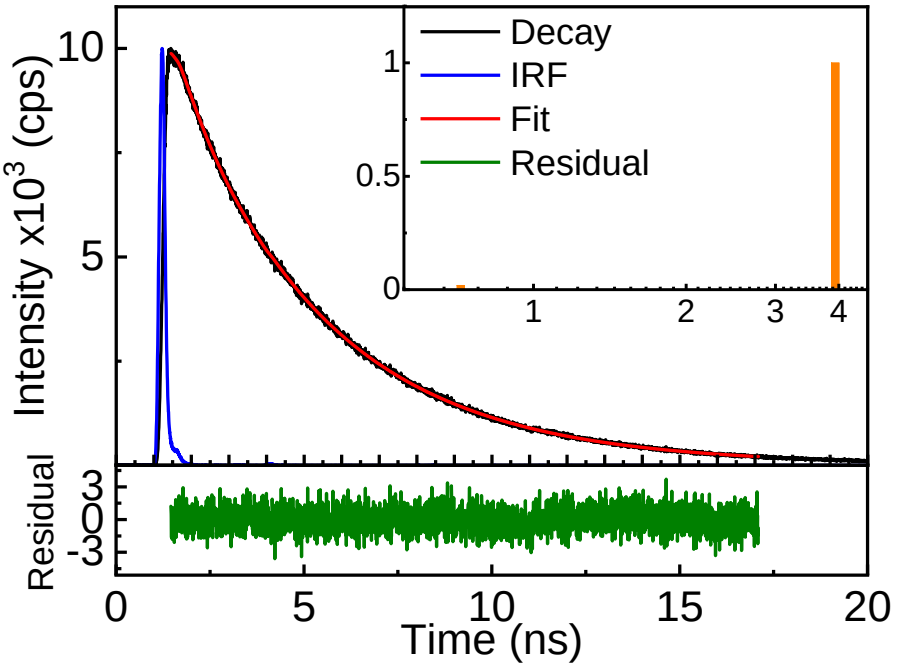

Figure S23: Emission decay (black) of $PC_{71}BM$ in solution in DCM at 298K, residuals (green), IRF (blue) and best fit (red). Multi-exponential analysis yields τ_P = 0.719 ns (1.8%), 3.937 ns (98.2%), χ^2 = 1.025. Inset, Multi-exponential analysis. λ_{ex}= 460 nm, λ_{em} = 532 nm.

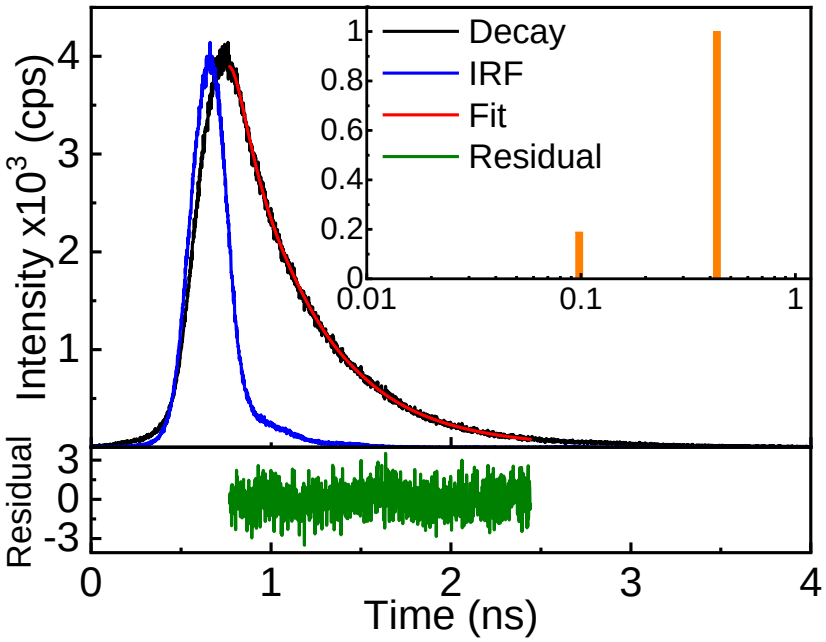

Figure S24: Emission decay (black) of P2 in solution in DCM at 298K, residuals (green), IRF (blue) and best fit (red). Multi-exponential analysis yields τ_P = 0.098 ns (16.4%), 0.431 ns (83.6%), χ^2 = 1.034. Inset, Multi-exponential analysis. λ_{ex}= 633 nm, λ_{em} = 712 nm.

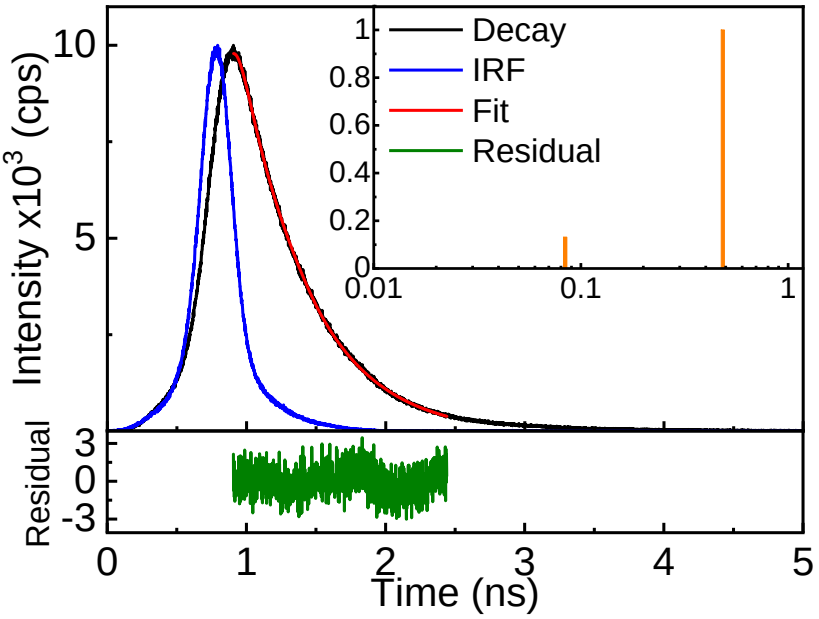

Figure S25: Emission decay (black) of a P2:MCzD blend (1:1) in solution in DCM at 298K, residuals (green), IRF (blue) and best fit (red). Multi-exponential analysis yields τ_P = 0.084 ns (11.6%), 0.484 ns (88.4%), χ^2 = 1.226. Inset, Multi-exponential analysis. λ_{ex}= 633 nm, λ_{em} = 712 nm.

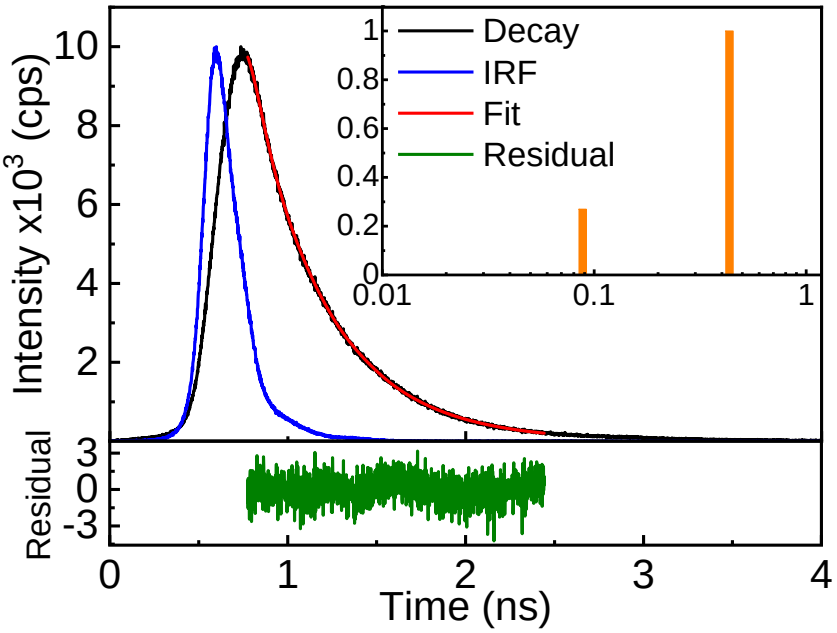

Figure S26: Emission decay (black) of a P2:MCzM blend (1:1) in solution in DCM at 298K, residuals (green), IRF (blue) and best fit (red). Multi-exponential analysis yields τ_P = 0.262 ns (38.1%), 1.009 ns (61.9%), χ^2 = 1.046. Inset, Multi-exponential analysis. λ_{ex}= 633 nm, λ_{em} = 712 nm.

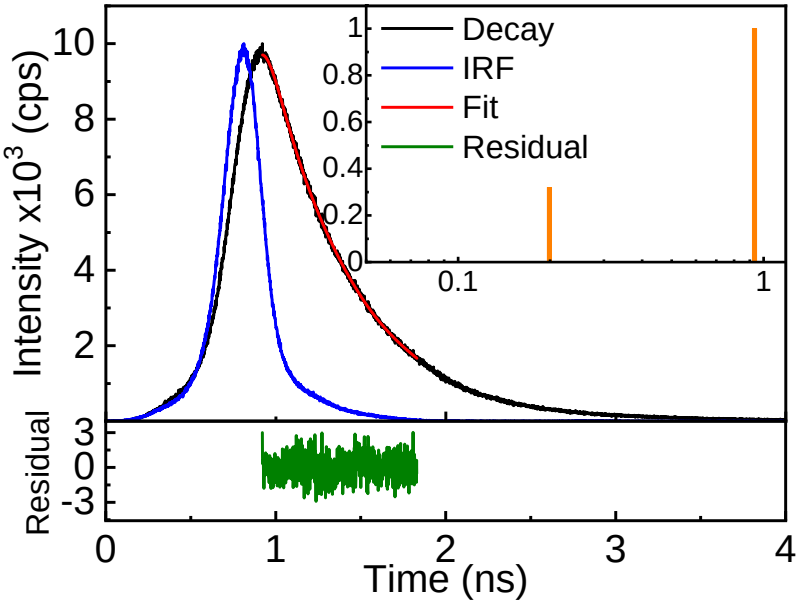

Figure S27: Emission decay (black) of a P2:$PC_{61}BM$ blend (1:1) in solution in DCM at 298K, residuals (green), IRF (blue) and best fit (red). Multi-exponential analysis yields τ_P = 0.199 ns (24.2%), 0.933 ns (75.8%), χ^2 = 1.079. Inset, Multi-exponential analysis. λ_{ex}= 633 nm, λ_{em} = 712 nm.

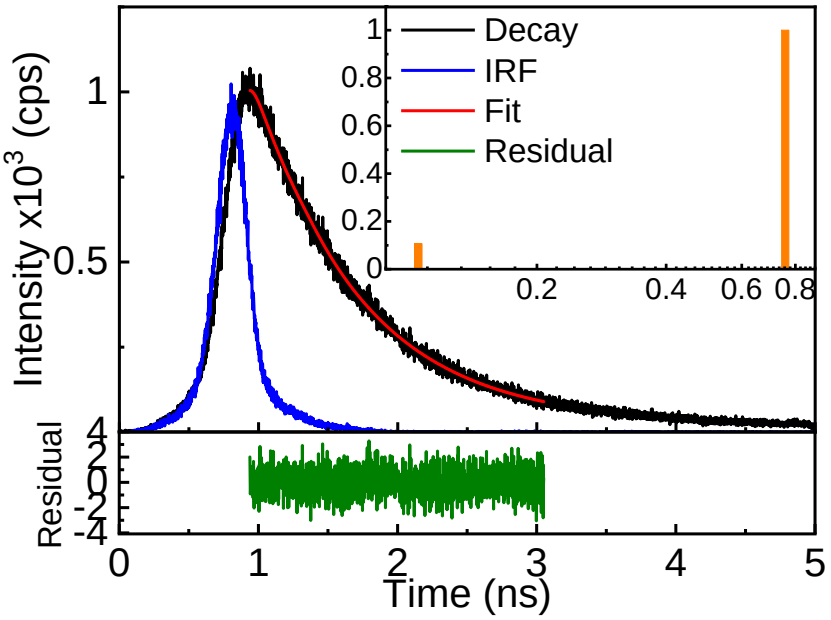

Figure S28: Emission decay (black) of a P2:$PC_{71}BM$ blend (1:1) in solution in DCM at 298K, residuals (green), IRF (blue) and best fit (red). Multi-exponential analysis yields τ_P = 0.106 ns (6.7%), 0.758 ns (93.3%), χ^2 = 1.006. Inset, Multi-exponential analysis. λ_{ex}= 633 nm, λ_{em} = 712 nm.

References

(1) Frisch, M. J.; Trucks, G. W.; Schlegel, H. E.; Scuseria, G. E.; Robb, M. A.; Cheeseman, J. R.; Scalmani, G.; Barone, V.; Petersson, G. A.; O., F.; Foresman, J. B.; Fox, J. D. Gaussian 16. *Gaussian, Inc., Wallingford CT*, **2016**, *3*.

(2) Hohenberg, P.; Kohn, W. Inhomogeneous Electron Gas. *Phys. Rev.* **1964**, *136* (3B), B864–B871. https://doi.org/10.1103/PhysRev.136.B864.

(3) Kohn, W.; Sham, L. J. Self-Consistent Equations Including Exchange and Correlation Effects. *Phys. Rev.* **1965**, *140* (4A), A1133–A1138. https://doi.org/10.1103/PhysRev.140.A1133.

(4) Gey, E. *Density-Functional Theory of Atoms and Molecules*; Oxford University Press, 1995; Vol. 191. https://doi.org/10.1524/zpch.1995.191.part_2.277a.

(5) SALAHUB, D. R.; ZERNER, M. C. ChemInform Abstract: The Challenge of d and f Electrons. Theory and Computation. In *ChemInform*; Salahub, D. R., Zerner, M. C., Eds.; ACS Symposium Series; American Chemical Society: Washington, DC, 1990; Vol. 21. https://doi.org/10.1002/chin.199033368.

(6) Bauernschmitt, R.; Ahlrichs, R. Treatment of Electronic Excitations within the Adiabatic Approximation of Time Dependent Density Functional Theory. *Chem. Phys. Lett.* **1996**, *256* (4–5), 454–464. https://doi.org/10.1016/0009-2614(96)00440-X.

(7) Casida, M. E.; Jamorski, C.; Casida, K. C.; Salahub, D. R. Molecular Excitation Energies to High-Lying Bound States from Time-Dependent Density-Functional Response Theory: Characterization and Correction of the Time-Dependent Local Density Approximation Ionization Threshold. *J. Chem. Phys.* **1998**, *108* (11), 4439–4449. https://doi.org/10.1063/1.475855.

(8) Stratmann, R. E.; Scuseria, G. E.; Frisch, M. J. An Efficient Implementation of Time-Dependent Density-Functional Theory for the Calculation of Excitation Energies of Large Molecules. *J. Chem. Phys.* **1998**, *109* (19), 8218–8224. https://doi.org/10.1063/1.477483.

(9) Lee, C.; Yang, W.; Parr, R. G. Development of the Colle-Salvetti Correlation-Energy Formula into a Functional of the Electron Density. *Phys. Rev. B* **1988**, *37* (2), 785–789. https://doi.org/10.1103/PhysRevB.37.785.

(10) Miehlich, B.; Savin, A.; Stoll, H.; Preuss, H. Results Obtained with the Correlation Energy Density Functionals of Becke and Lee, Yang and Parr. *Chem. Phys. Lett.* **1989**, *157* (3), 200–206. https://doi.org/10.1016/0009-2614(89)87234-3.

(11) Pritchard, B. P.; Altarawy, D.; Didier, B.; Gibson, T. D.; Windus, T. L. New Basis Set Exchange: An Open, Up-to-Date Resource for the Molecular Sciences Community. *J. Chem. Inf. Model.* **2019**, *59* (11), 4814–4820. https://doi.org/10.1021/acs.jcim.9b00725.

(12) O'Boyle, N. M.; Tenderholt, A. L.; Langner, K. M. Cclib: A Library for Package-Independent Computational Chemistry Algorithms. *J. Comput. Chem.* **2008**, *29* (5), 839–845. https://doi.org/10.1002/jcc.20823.